Article

Spectroscopic Characterization of Photolytically Generated Radical Ion Pairs in Single-Wall Carbon Nanotubes Bearing Surface-Immobilized Tetrathiafulvalenes

M. ngeles Herranz, Christian Ehli, Stphane Campidelli, Miriam Gutirrez, Gordon L. Hug, Kei Ohkubo, Shunichi Fukuzumi, Maurizio Prato, Nazario Martn, and Dirk M. Guldi

J. Am. Chem. Soc., **2008**, 130 (1), 66-73 • DOI: 10.1021/ja073975t

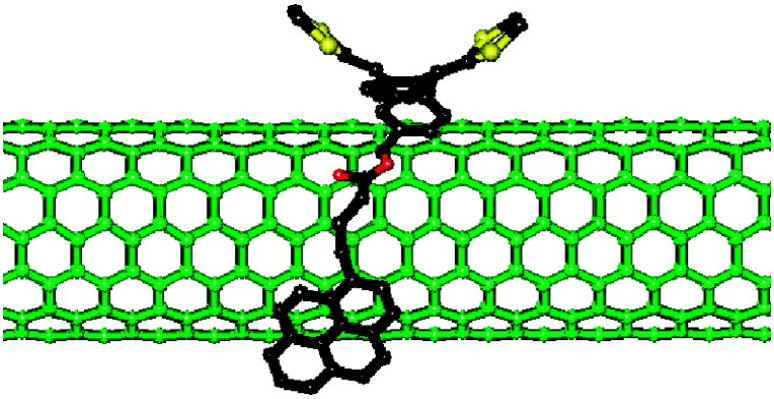

More About This Article

Additional resources and features associated with this article are available within the HTML version:

- Supporting Information
- Links to the 10 articles that cite this article, as of the time of this article download
- Access to high resolution figures
- Links to articles and content related to this article
- Copyright permission to reproduce figures and/or text from this article

View the Full Text HTML

J|A|C|S
ARTICLES
Published on Web 12/08/2007

Spectroscopic Characterization of Photolytically Generated Radical Ion Pairs in Single-Wall Carbon Nanotubes Bearing Surface-Immobilized Tetrathiafulvalenes

M. Ángeles Herranz,[†] Christian Ehli,[‡] Stéphane Campidelli,[§] Miriam Gutiérrez,[†] Gordon L. Hug,[⊥] Kei Ohkubo,[#] Shunichi Fukuzumi,*[,#] Maurizio Prato,*[,§] Nazario Martín,*[,†] and Dirk M. Guldi*[,‡]

Contribution from the Departamento de Química Orgánica I, Facultad de Química, Universidad Complutense de Madrid, E-28040 Madrid, Spain, Department of Chemistry and Pharmacy Interdisciplinary Center for Molecular Materials (ICMM), Friedrich-Alexander-Universität Erlangen-Nürnberg, Egerlandstrasse 3, 91058 Erlangen, Germany, Dipartimento di Scienze Farmaceutiche, Università di Trieste, Piazzale Europa, 1, 34127 Trieste, Italy, Radiation Laboratory, University of Notre Dame, Notre Dame, Indiana 46556, and Department of Material and Life Science, Graduate School of Engineering, Osaka University, SORST, (JST) Osaka 565-0871, Japan

Received June 1, 2007; E-mail: nazmar@quim.ucmes; dirk.guldi@chemie.uni-erlanger.de; prato@units.it; fukuzumi@chem.eng.osaka-u.ac.jp

Abstract: We succeeded in establishing for the first time a conclusive spectroscopic signature for reduced single-wall carbon nanotubes (SWNT), which evolves from electron donor−acceptor interactions between SWNT and electron-donating π-extended tetrathiafulvalene (exTTF). In particular, $\pi-\pi$ interactions were employed to anchor the electron donor to the surface of SWNT. New conduction band electrons, injected from photoexcited exTTF, shift the transitions that are associated with the van Hove singularities to lower energies.

Introduction

Nanometer-scale structures are of considerable interest for the development of optoelectronic applications. The unique and remarkable features of such architectures are primarily determined by their size, shape, composition, and structure.[1] An important trend in this field is based on the recent developments of photocurrent generating devices, where molecular hybrids—organic and/or inorganic—as nanometer-scale prototypes are at the forefront. Among the new nanomaterials that have exerted a profound impact on fundamental and technological issues, carbon nanotubes (CNT) stand out owing to their extraordinary electronic and mechanical properties.[2]

The development of reliable and reproducible methodologies to integrate CNT into functional structures—such as donor−acceptor hybrids, able to transform sunlight into electrical or chemical energy—has emerged as an area of intense research.[3,4] This is largely due to the unique electronic properties exhibited by these carbon allotropes and their prospects for practical applications.[5]

Since small band gaps characterize most semiconducting single-wall carbon nanotubes (SWNT)—less than 1 eV—these components are capable of functioning either as electron acceptors or electron donors.[6] In fact, recent work has provided experimental evidence in support of either electron-transfer reactivity.[7,8] Scattered results—both experimental and theoretical—

[†] Universidad Complutense de Madrid.
[‡] Friedrich-Alexander-Universität Erlangen-Nürnberg.
[§] Università di Trieste.
[⊥] University of Notre Dame.
[#] Osaka University.

(1) (a) Fritzsche, W.; Köhler, M. *Nanotechnology: An Introduction to Nanostructuring Techniques*; Wiley: Weinheim, Germany, 2004. (b) Rao, C. *Chemistry of Nanomaterials: Synthesis, Properties and Applications*; Wiley: Weinheim, Germany, 2004. (c) Wolf, E. *Nanophysics and Nanotechnology: An Introduction to Modern Concepts in Nanoscience*; Wiley: Weinheim, Germany, 2004. (d) Cao, G. *Nanostructures and Nanomaterials: Synthesis, Properties & Applications*; Imperial College: London, 2004.

(2) (a) *Carbon Nanotubes and Related Structures: New Materials for the Twenty-First Century*; Harris, P., Ed.; Cambridge University Press: Cambridge, 2001. (b) Sgobba, V.; Rahman, G. M. A.; Ehli, C.; Guldi, D. M. In *Covalent and Non-Covalent Approaches Towards Multifunctional Carbon Nanotube Materials—Fullerenes*; Langa de la Puente, F., Nierengarten, J. F., Eds.; RSC Nanoscience and Nanotechnology Series; Cambridge, United Kingdom, 2007. (c) Sgobba, V.; Rahman, G. M. A.; Guldi, D. M. Carbon Nanotubes in Electron Donor−Acceptor Nanocomposites. In *Chemistry of Carbon Nanotubes*; Basiuk, V. A., Ed.; American Scientific Publishers: Stevenson Ranch, CA, 2006. (d) Reich, S.; Thomsen, C.; Maultzsch, J. *Carbon Nanotubes: Basic Concepts and Physical Properties*; VCH: Weinheim, Germany, 2004. (e) *Acc. Chem. Res.* **2002**, *35* (Special Issue), 997−1113.

(3) (a) *Carbon Nanotubes: Synthesis, Structure, Properties and Applications*; Dresselhaus, M. S., Dresselhaus, G., Avouris P., Eds.; Springer: Berlin, 2001. (b) Reich, S.; Thomsen, C.; Maultzsch, J. *Carbon Nanotubes: Basic Concepts and Physical Properties*; Wiley-VCH: Weinheim, Germany, 2004. (c) Popov, V. N.; Lambin, P. *Carbon Nanotubes*; Springer: Dordrecht, The Netherlands, 2006. (d) *Interface* **2006**, *15* (Special Issue), 23−65.

(4) For reviews, see: (a) Hirsch, A. *Angew. Chem., Int. Ed.* **2002**, *41*, 1853−1859. (b) Barh, J. L.; Tour, J. M. *J. Mater. Chem.* **2002**, *12*, 1952−1958. (c) Nigoyi, S.; Hamon, M. A.; Hu, H.; Zhao, B.; Bhomwik, P.; Sen, R.; Itkis, M. E.; Haddon, R. C. *Acc. Chem. Res.* **2002**, *35*, 1105−1013. (d) Sun, Y.-P.; Fu, K.; Lin, Y.; Huang, W. *Acc. Chem. Res.* **2002**, *35*, 1096−1104. (e) Banerjee, S.; Kahn, M. G. C.; Wong, S. S. *Chem. Eur. J.* **2003**, *9*, 1898−1908. (f) Tasis, D.; Tagmatarchis, N.; Georgakilas, V.; Prato, M. *Chem. Eur. J.* **2003**, *9*, 4001−4008. (g) Dyke, C. A.; Tour, J. M. *Chem. Eur. J.* **2004**, *10*, 812−817. (h) Banerjee, S.; Hemraj-Benny, T.; Wong, S. S. *Adv. Mater.* **2005**, *17*, 17−29. (i) Guldi, D. M.; Rahman, G. M. A.; Zerbetto, F.; Prato, M. *Acc. Chem. Res.* **2005**, *38*, 871−878. (j) Tasis, D.; Tagmatarchis, N.; Bianco, A. *Chem. Rev.* **2006**, *106*, 1105−1136. (k) Guldi, D. M.; Rahman, G. M. A.; Sgobba, V.; Ehli, C. *Chem. Soc. Rev.* **2006**, *35*, 471−487. (l) Guldi, D. M. *Phys. Chem. Chem. Phys.* **2007**, 1400−1420.

 10.1021/ja073975t CCC: $40.75

suggest that changes in the features of the van Hove singularities, the visible−near-infrared (vis−NIR) absorption bands typical of HiPCO SWNT, might be associated with electron transfer.[9] In a recent contribution,[9b] SWNT were radiolytically reduced revealing a negative imprint, that is, bleaching of the van Hove singularities. One of the aims of the work described herein was to establish a spectroscopic signature of reduced SWNT,[10] which can be widely applicable to future tests on electron donor−acceptor interactions with SWNT.

Covalent functionalization of SWNT with electron donors either requires extensive sonication and use of strongly oxidizing agents or generates partial saturation of the extended π-system.[11] As a consequence, major changes occur on the π-electronic properties and likewise their spectroscopic identity.[12] An alternative strategy to control the organization between donor and acceptor units, while preserving the π-electronic structure of SWNT, is the supramolecular functionalization of SWNT by means of hydrophobic, π-stacking, or van der Waals interactions with the sidewalls of SWNT. The noncovalent attachment of aromatic species to the nanotube surface has been widely investigated, using conjugated polymers,[13] as well as pyrene,[14−16] anthracene,[17] and porphyrin derivatives.[18,19]

As a suitable electron donor, we turned to π-extended tetrathiafulvalene (exTTF)[20]—a selection that is driven by its strong electron donor character. Contrary to metalloporphyrins or metallophthalocyanines, which, upon excitation can act both as strong donors and as weak acceptors, exTTF can only behave as a donor. Therefore, the result of photoinduced electron transfer can only generate holes in exTTF and electrons in SWNT. Thus, our strategy involves the design and synthesis of a bifunctional molecule, pyrene−exTTF (Scheme 1). The use of pyrene derivatives is particularly crucial to achieve surface immobilization onto SWNT through directed $\pi-\pi$ interactions.[14] We also emphasize that pyrene functions exclusively as an anchor that guarantees the immobilization of the electron donor (i.e., exTTF) onto the SWNT surface. We present here a detailed and unambiguous spectroscopic investigation that sheds light onto the changes that electron transfer induces on the van Hove singularities in semiconducting SWNT.

Results and Discussion

The synthesis of the new pyrene−exTTF molecule is based on the covalent linkage of both redox-active units through a flexible and medium-length chain (six atoms) which favors a facile interaction with the SWNT surface. Pyrene−exTTF was prepared by esterification of 2-(hydroxymethyl)-9,10-bis(1,3-dithiol-2-ylidine)-9,10-dihydroanthracene,[21] hereafter referred to as exTTF, with 1-pyrenebutyric acid in the presence of 1,3-dicyclohexylcarbodiimide (DCC)/4-(dimethylamino)-pyridine (DMAP) (Scheme 1). To prepare the SWNT/pyrene−exTTF ensemble, 2 mg of SWNT and 1 mg of pyrene−exTTF were suspended in 4 mL of THF. The mixture was kept overnight under vigorous stirring, then it was sonicated (112 W) for 45 min. During this process the temperature was kept constant at 20 °C. To minimize the amount of free pyrene−exTTF in

(5) (a) Tans, S. J.; Devoret, M. H.; Dai, H.; Thess, A.; Smalley, R. E.; Geerligs, L. J.; Dekker, C. *Nature* **1997**, *386*, 474−477. (b) Tans, S. J.; Verschnesen, A. R. M.; Dekker, C. *Nature*, **1998**, *393*, 49−52. (c) Paulson, S.; Helsen, A.; Buongiorno, N. M.; Taylor, R. M.; Falvo, M.; Superfine, R.; Washburn, S. *Science* **2000**, *290*, 1942−1949. (d) O'Connel, M. J.; Bachilo, S. M.; Huffmann, C. B.; Moore, V. C.; Strano, M. S.; Haroz, E. H.; Rialon, K. L.; Boul, P. J.; Noon, W. H.; Kittrell, C.; Hauge, J. M. R. H.; Weisman, R. B.; Smalley, R. E. *Science*, **2002**, *297*, 593−596. (e) Dalton, A. B.; Collins, S.; Muñoz, E.; Razal, J. M.; Ebron, V. H.; Ferraris, J. P.; Coleman, J. N.; Kim, B. G.; Baughman, R. H. *Nature* **2003**, *423*, 703−703. (f) Javey, A.; Guo, J.; Wang, Q.; Lundstrom, M.; Dai, H. J. *Nature* **2003**, *423*, 654−657.

(6) (a) Heller, I.; Kong, J.; Williams, K. A.; Dekker, C.; Lemay, S. G. *J. Am. Chem. Soc.* **2006**, *128*, 7353−7359. (b) Heller, I.; Kong, J.; Heering, H. A.; Williams, K. A.; Lemay, S. G.; Dekker, C. *Nano Lett.* **2005**, *5*, 137−142. (c) Day, T. M.; Wilson, N. R.; Macpherson, J. V. *J. Am. Chem. Soc.* **2004**, *126*, 16724−16725. (d) Ehli, C.; Rahman, G. M. A.; Jux, N.; Balbinot, D.; Guldi, D. M.; Paolucci, F.; Marcaccio, M.; Paolucci, D.; Melle-Franco, M.; Zerbetto, F.; Campidelli, S.; Prato, M. *J. Am. Chem. Soc.* **2006**, *128*, 11222−11231.

(7) (a) Guldi, D. M.; Marcaccio, M.; Paolucci, D.; Paolucci, F.; Tagmatarchis, N.; Tasis, D.; Vázquez, E.; Prato, M. *Angew. Chem., Int. Ed.* **2003**, *42*, 4206−4209. (b) Li, H.; Martin, R. B.; Harruff, B. A.; Carino, R. A.; Allard, L. F.; Sun, Y.-P. *Adv. Mater.* **2004**, *16*, 896−900. (c) Guldi, D. M.; Rahman, G. M. A.; Ramey, J.; Marcaccio, M.; Paolucci, D.; Paolucci, F.; Qin, S.; Ford, W. T.; Balbinot, D.; Jux, N.; Tagmatarchis, N.; Prato, M. *Chem. Commun.* **2004**, 2034−2035. (d) Guldi, D. M.; Taieb, H.; Rahman, G. M. A.; Tagmatarchis, N.; Prato, M. *Adv. Mater.* **2005**, *17*, 871−875. (e) Guldi, D. M.; Rahman, G. M. A.; Prato, M.; Jux, N.; Qin, S.; Ford, W. *Angew. Chem., Int. Ed.* **2005**, *44*, 2015−2018. (f) Baskaran, D.; Mays, J. W.; Zhang, X. P.; Bratcher, M. S. *J. Am. Chem. Soc.* **2005**, *127*, 6916−6917. (g) Rahman, G. M. A.; Guldi, D. M.; Cagnoli, R.; Mucci, A.; Schenetti, L.; Vaccari, L.; Prato, M. *J. Am. Chem. Soc.* **2005**, *127*, 10051−10057. (h) Guldi, D. M.; Rahman, G. M. A.; Qin, S.; Tchoul, M.; Ford, W. T.; Marcaccio, M.; Paolucci, D.; Paolucci, F.; Campidelli, S.; Prato, M. *Chem. Eur. J.* **2006**, *12*, 2152−2161. (i) Alvaro, M.; Atienzar, P.; de la Cruz, P.; Delgado, J. L.; Troiani, V.; García, H.; Langa, F.; Palkar, A.; Echegoyen, L. *J. Am. Chem. Soc.* **2006**, *128*, 6626−6635. (j) Campidelli, S.; Sooambar, C.; Lozano-Diz, E.; Ehli, C.; Guldi, D. M.; Prato, M. *J. Am. Chem. Soc.* **2006**, *128*, 12544−12552.

(8) (a) Hecht, D. S.; Ramirez, R. J. A.; Briman, M.; Artukovic, E.; Chichak, K. S.; Stoddart, J. F.; Gruner, G. *Nano Lett.* **2006**, *6*, 2031−2036. (b) Rao, A. M.; Eklund, P. C.; Bandow, S.; Thess, A.; Smalley, R. E. *Nature* **1997**, *388*, 257−259.

(9) (a) Herranz, M. A.; Martín, N.; Campidelli, S.; Prato, M.; Brehm, G.; Guldi, D. M. *Angew. Chem., Int. Ed.* **2006**, *45*, 4478−4482. (b) Guldi, D. M.; Rahman, G. M. A.; Rahman Sgobba, V.; Bonifazi, D.; Prato, M.; Kotov, N. A. *J. Am. Chem. Soc.* **2006**, *128*, 2315−2323. (c) Melle-Franco, M.; Marcaccio, M.; Paolucci, F.; Georgakilas, V.; Guldi, D. M.; Prato, M.; Zerbetto, F. *J. Am. Chem. Soc.* **2004**, *126*, 1646−1647.

(10) X-ray photoemission spectroscopy (XPS) and near-edge X-ray-absorption fine structure (NEXAFS) spectroscopy signatures of carrier-doped SWNT have been investigated. See: Shiraishi, M.; Swaraj, S.; Takenobu, T.; Iwasa, Y.; Ata, M.; Unger, W. E. S. *Phys. Rev. B* **2005**, *71*, 125419.

(11) (a) See, for example: Holzinger, M.; Hirsch, A.; Bernier, P.; Duesberg, G. S.; Burghard, M. *Appl. Phys. A* **2000**, *70*, 599−602. (b) Georgakilas, V.; Kordatos, K.; Prato, M.; Guldi, D. M.; Holzinger, M.; Hirsch, A. *J. Am. Chem. Soc.* **2002**, *124*, 760.

(12) (a) Strano, M. S.; Dyke, C. A.; Usrey, M. L.; Barone, P. W.; Allen, M. J.; Shan, H.; Kittrell, C.; Hauge, R. H.; Tour, J. M.; Smalley, R. E. *Science* **2003**, *301*, 1519−1522. (b) Zurek, E.; Autschbach, J. *J. Am. Chem. Soc.* **2004**, *126*, 13079−13088.

(13) (a) Star, A.; Stoddart, J. F.; Steuerman, D.; Diehl, M.; Boukai, A.; Wong, E. W.; Yang, X.; Chung, S. W.; Choi, H.; Heath, J. R. *Angew. Chem., Int. Ed.* **2001**, *40*, 1721−1725. (b) Chen, J.; Liu, H. Y.; Weimer, W. A.; Halls, M. D.; Waldeck, D. H.; Walker, G. C. *J. Am. Chem. Soc.* **2002**, *124*, 9034−9035. (c) Gomez, F. J.; Chen, R. J.; Wang, D. W.; Waymouth, R. M.; Dai, H. J. *Chem. Commun.* **2003**, 190−191.

(14) Chen, R. J.; Zhang, Y.; Wang, D.; Dai, H. *J. Am. Chem. Soc.* **2001**, *123*, 3838−3839.

(15) Nakashima, N.; Tomonari, Y.; Murakami, H. *Chem. Lett.* **2002**, 638−639.

(16) (a) Petrov, P.; Stassin, F.; Pagnoulle, C.; Jerome, R. *Chem. Commun.* **2003**, 2904−2905. (b) Liu, L.; Wang, T. X.; Li, J. X.; Guo, Z. X.; Dai, L. M.; Zhang, D. Q.; Zhu, D. B. *Chem. Phys. Lett.* **2003**, *367*, 747−752.

(17) Zhang, J.; Lee, J. K.; Wu, Y.; Murray, R. W. *Nano Lett.* **2003**, *3*, 403−407.

(18) For recent examples, see: (a) Guldi, D. M.; Rahman, G. M. A.; Jux, N.; Balbinot, D.; Hartnagel, U.; Tagmatarchis, N.; Prato, M. *J. Am. Chem. Soc.* **2005**, *127*, 9830−9838. (b) Hasobe, T.; Fukuzumi, S.; Kamat, P. V. *J. Am. Chem. Soc.* **2005**, *127*, 11884−11885. (c) Satake, A.; Miyajima, Y.; Kobuke, Y. *Chem. Mater.* **2005**, *17*, 716−724. (d) Sgobba, V.; Rahman, G. M. A.; Guldi, D. M.; Jux, N.; Campidelli, S.; Prato, M. *Adv. Mater.* **2006**, *18*, 2264−2269.

(19) Li, H.; Zhou, B.; Lin, Y.; Gu, L.; Wang, W.; Fernando, K. A. S.; Kumar, S.; Allard, L. F.; Sun, Y.-P. *J. Am. Chem. Soc.* **2004**, *126*, 1014−1015.

(20) For representative C_{60}–exTTF conjugates, see: (a) Martín, N.; Sánchez, L.; Guldi, D. M. *Chem. Commun.* **2000**, 113−114. (b) Herranz, M. A.; Martín, N.; Ramey, J.; Guldi, D. M. *Chem. Commun.* **2002**, 2968−2969. (c) Sánchez, L.; Pérez, I.; Martín, N.; Guldi, D. M. *Chem. Eur. J.* **2003**, *9*, 2457−2468. (d) Giacalone, F.; Segura, J. L.; Martín, N.; Guldi, D. M. *J. Am. Chem. Soc.* **2004**, *126*, 5340−5341. (e) Giacalone, F.; Martín, N.; Ramey, J.; Guldi, D. M. *Chem. Eur. J.* **2005**, *11*, 4819−4834. (f) Handa, S.; Giacalone, F.; Haque, S. A.; Palomares, E.; Martín, N.; Durrant, J. R. *Chem. Eur. J.* **2005**, *11*, 7440−7447. (g) Sánchez, L.; Sierra, M.; Martín, N.; Guldi, D. M.; Wienk, M. W.; Janssen, R. A. J. *Org. Lett.* **2005**, *128*, 1048−10490. (h) Martín, N. *Chem. Commun.* **2006**, 2093−2104. (i) Atienza, C.; Martín, N.; Wielopolski, M.; Haworth, N.; Clark, T.; Guldi, D. M. *Chem. Commun.* **2006**, 3202−3204.

(21) González, S.; Martín, N.; Guldi, D. M. *J. Org. Chem.* **2003**, *68*, 779−791.

Scheme 1. Synthesis of Pyrene−exTTF and Supramolecular SWNT/Pyrene−exTTF Nanohybrids

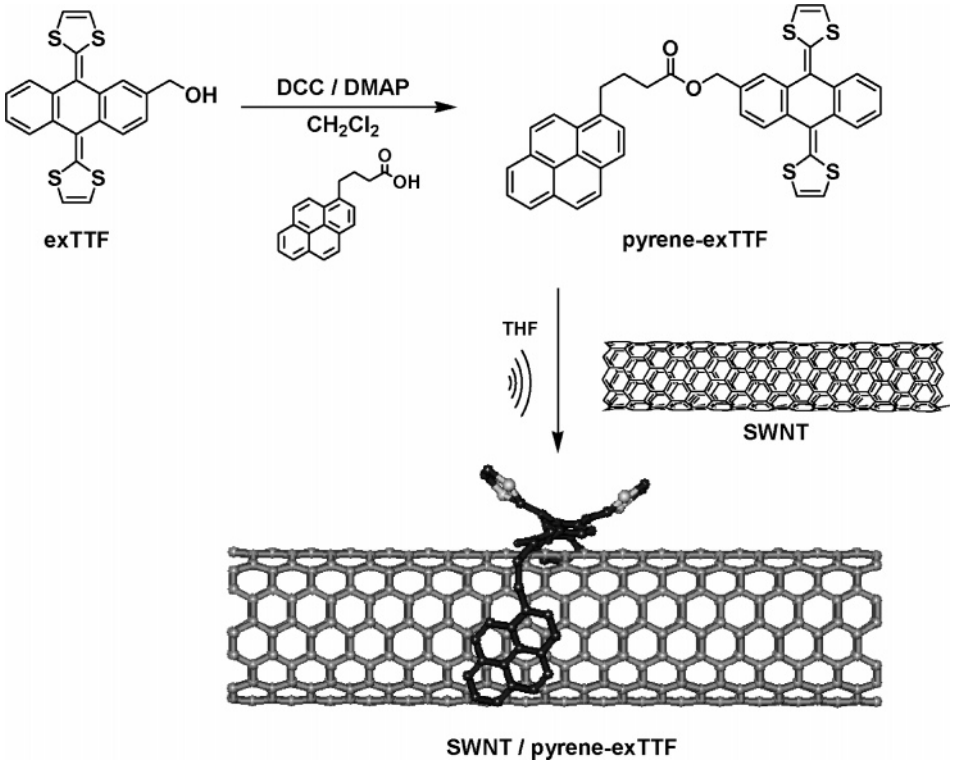

solution, the sample of SWNT/pyrene−exTTF was centrifuged at 6000 rpm for 20 min and the supernatant was removed. The remaining solid, free of pyrene−exTTF excess, was resuspended in THF for further characterization.

Standard analytical and spectroscopic techniques—UV−vis−NIR spectroscopy, thermogravimetric analysis (TGA), electrochemistry, transmission electron microscopy (TEM), and atomic force microscopy (AFM)—were employed to characterize the new nanohybrid. In complementary work, the photophysical properties were obtained by steady-state and time-resolved fluorescence as well as femtosecond transient absorption spectroscopy.

The amount of SWNT-immobilized pyrene−exTTF was estimated by TGA. For SWNT/pyrene−exTTF the weight loss is approximately 5% at 600 °C. At the same temperature, pyrene−exTTF reveals a loss of 70% (Figure 1). With this data in hand, we estimate that a complete destruction of pyrene−exTTF in SWNT/pyrene−exTTF would cause a loss of weight of about 7%, which corresponds to a ratio of a single pyrene−exTTF per 750 carbon atoms of SWNT.[22] The presence of pyrene−exTTF on the SWNT in the nanohybrid precipitate gives additional proof that pyrene moieties are strongly anchored on the nanotube sidewalls. Notable is that the supramolecular interactions between SWNT and pyrene−exTTF leave the electronic structure of SWNT intact. In particular, Raman experiments (i.e., 1064 nm excitation), which reveal no appreciable shifts of the radial breathing mode (RBM) band or intensification of the D-bands,[23] upon normalization to the G-band, support this notion (Supporting Information Figure S1).

Structural details of SWNT/pyrene−exTTF nanohybrids were obtained by TEM and AFM measurements (Figure 2). Common to TEM and AFM images is high aspect ratio objects that appear throughout the scanned regions. From TEM, SWNT derivatives appear as thin bundles with mean lengths on the order of several micrometers. Typical AFM images revealed the presence of individual SWNT and thin bundles with diameters of about 1 nm and 3−10 nm, respectively. Overall, AFM images of SWNT/pyrene−exTTF resemble those registered upon scanning SWNT that are dispersed with amphiphilic pyrene derivatives.[18a] This

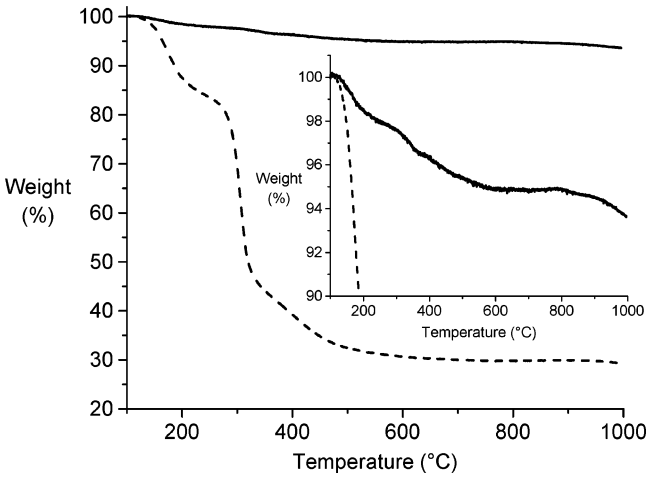

Figure 1. Thermogravimetric analysis of pyrene−exTTF (dashed line) and SWNT/pyrene−exTTF (solid line).

(22) We estimated the functionalization of SWNT with pyrene−exTTF to 7% (5%/70%). The SWNT/pyrene−exTTF nanohybrids are constituted roughly of 93% of carbon (from nanotubes) and 7% of exTTF derivative; the amount of functional group is $(93/M_C)/(7/M_{\text{Pyrene-exTTF}}) \approx 750$. The low ratio is likely due to the solubility of pyrene−exTTF in THF. Obviously, we formulate a competition between the SWNT immobilization and the complete solubilization by the solvent. The mechanism is quite different from the case noted for amphiphilic pyrene derivatives that we used in previous work, where a ratio of 1 to 280 carbon atoms was extrapolated (ref 6d): Amphiphilic pyrene derivatives form aggregates in water and in the presence of SWNT; the association of the apolar moiety with the SWNT sidewall results in a gain of energy leading to a stable suspension.

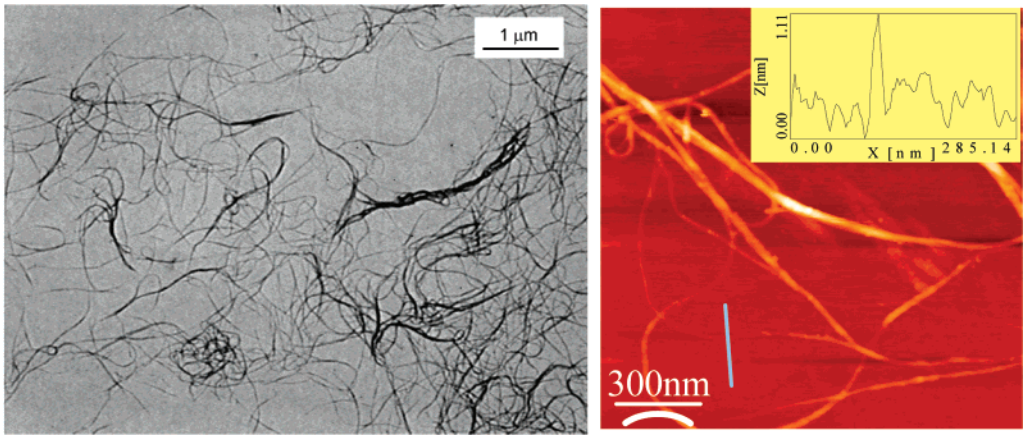

Figure 2. Images of SWNT/pyrene−exTTF nanohybrid. Left: TEM image showing small bundles of nanotubes well-dispersed on the grid. Right: AFM image showing thin bundles as well as isolated tubes with diameters of about 1 nm.

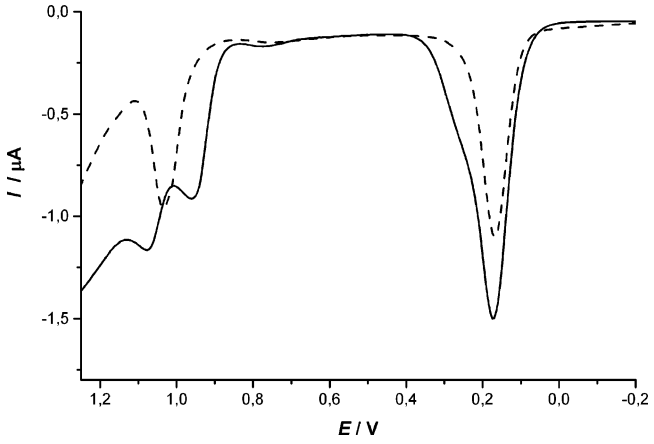

Figure 3. OSWVs obtained for the pyrene−exTTF molecule (0.5 mM) (dashed line) and a SWNT/pyrene−exTTF mixture (solid line) (saturated solution) in a 0.1 M $TBAClO_4$–CH_2Cl_2 solution. $\upsilon = 500$ mV/s, $T = 25$ °C; working electrode, glassy carbon; reference electrode, $Ag/AgNO_3$; counter electrode, Pt wire.

confirms the successful inmobilization of pyrene−exTTF onto the surface of SWNT.

The electrochemical properties of pyrene−exTTF and SWNT/pyrene−exTTF were investigated in solutions of CH_2Cl_2 and THF containing 0.1 M $TBAClO_4$ under inert conditions (i.e., saturated argon atmosphere). The SWNT/pyrene−exTTF mixtures were prepared by combining weight equivalents of SWNT and pyrene−exTTF in CH_2Cl_2 or THF. The samples were kept for several hours while stirring vigorously, after which they were sonicated and filtered for electrochemical analysis. Although SWNT/pyrene−exTTF were prepared successfully in both solvents, the rather limited potential range that is available for measurements in THF—especially in the anodic range—prevents the observation of some of the oxidation processes. Consequently, we have set our focus to CH_2Cl_2 as a solvent.

The cyclic (CV) and Osteryoung square wave voltammograms (OSWV) of the pyrene−exTTF derivative exhibit two peaks at +170 and +1035 mV, respectively (Figure 3). The first oxidation peak corresponds to the single two-electron and chemically reversible oxidation process of exTTF,[24] whereas the second peak is due to the oxidation of the pyrene fragment.[25]

Upon comparison of SWNT/pyrene−exTTF with pyrene−exTTF, the following differences evolve. First, the exTTF-based oxidation, although appearing at exactly the same potential (i.e., +170 mV) is noticeably broader in SWNT/pyrene−exTTF. A likely rationale implies the presence of two coexisting species, namely, free pyrene−exTTF and SWNT-immobilized pyrene−exTTF, with little difference in oxidation potentials. Probably, the weak interactions between free and immobilized exTTF cause a small difference in oxidation potentials. Instead, the much stronger interactions between the pyrene unit and SWNT generates a larger shift (100 mV) in oxidation potential for the free and immobilized pyrene, with values of +1060 and +960 mV, respectively. Such an apparent stabilization of the pyrene radical cation—when interacting with SWNT—has been recently observed for similar systems.[6d,25]

Absorption spectra of SWNT/pyrene−exTTF taken in THF exhibit characteristics of all building blocks (i.e., SWNT, pyrene, and exTTF—see Figure 4) and also provide evidence for their mutual electronic interactions. For a sample of SWNT/pyrene−exTTF the typical vis−NIR absorption bands (van Hove singularities) extend throughout 1600 nm with peaks at 557, 599, 653, 741, 811, 876, 1213, 1320, and 1446 nm. Importantly, these maxima are significantly shifted to the red, when compared to those of SWNT suspensions in THF. The most significant differences are observed at 1208, 1313, and 1437 nm. Interestingly, for SWNT/1-hydroxymethylpyrene (i.e., a pyrene derivative with no exTTF) also red-shifts are seen (i.e., 1199, 1308, and 1441 nm), whereas SWNT/exTTF (i.e., lacking the pyrene tether) shows peaks at 556, 598, 652, 739, 812, 876, 1169, 1214, 1316, and 1444 nm. In other words, absorption spectroscopy further confirms the electrochemical conclusions that in SWNT/pyrene−exTTF interactions of SWNT with pyrene are appreciably stronger than those with exTTF. Finally, maxima at 243, 255, 266, 277, 314, 328, and 344 nm are assigned to the pyrene unit, whereas exTTF was identified through typical bands at 363 and 431 nm.

To evaluate excited-state interactions, as a complement to the above-described ground-state interactions, we investigated first the fluorescence spectroscopy. In particular, in the absence

(23) Marcolongo, G.; Ruaro, G.; Gobbo, M.; Meneghetti, M. *Chem. Commun*, **2007**, 4925−4927.
(24) Herranz, M. A.; Yu, L.; Echegoyen, L.; Martín, N. *J. Org. Chem.* **2003**, *68*, 8379−8385.
(25) Guldi, D. M.; Menna, E.; Maggini, M.; Marcaccio, M.; Paolucci, D.; Paolucci, F.; Campidelli, S.; Prato, M.; Rahman, G. M. A.; Schergna, S. *Chem. Eur. J.* **2006**, *12* 3975−3983.

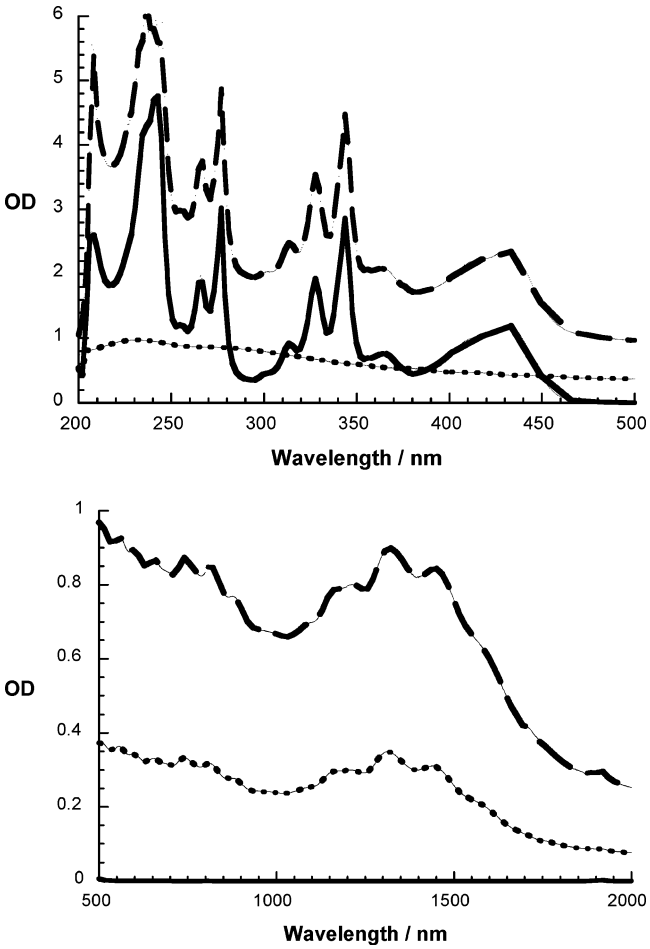

Figure 4. Upper part: absorption spectra (i.e., 200−500 nm) of pyrene−exTTF (solid line), SWNT (dotted line), and SWNT/pyrene−exTTF (dashed line) in THF. Lower part: absorption spectra (i.e., 500−2000 nm) of pyrene−exTTF (solid line), SWNT (dotted line), and SWNT/pyrene−exTTF (dashed line) in THF.

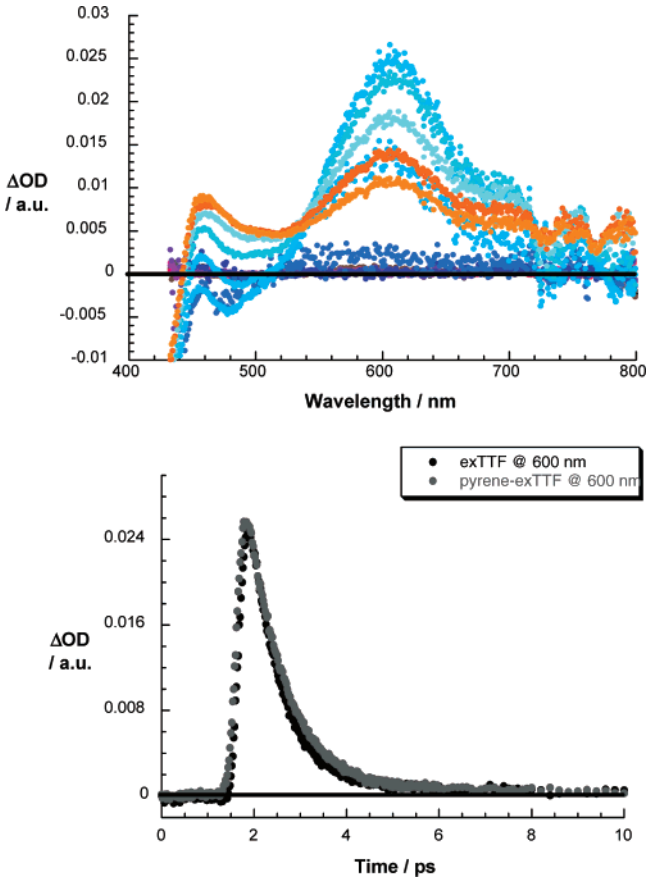

Figure 5. Upper part: differential absorption spectra (visible) obtained upon femtosecond flash photolysis (387 nm) of exTTF in THF with several time delays between 0 and 10 ps at room temperature. Lower part: time−absorption profiles of the spectra shown above at 600 nm, monitoring the decay of the exTTF excited state in exTTF and pyrene−exTTF.

of molecular oxygen, pyrene exhibits a fluorescence quantum yield close to unity and a fluorescence lifetime of nearly 100 ns. Notably, in pyrene−exTTF the fluorescence quantum yields (0.7) and fluorescence lifetimes (16 ns) of pyrene are somewhat affected, relative to pristine pyrene, by the presence of exTTF (under comparable conditions the fluorescence lifetime of pristine pyrene is 18 ns). Next, to compare pyrene−exTTF with SWNT/pyrene−exTTF we adjusted their solutions to exhibit equal absorbance at 344 nm. This wavelength of matching absorption was then used to photoexcite the pyrene moieties in pyrene−exTTF and SWNT/pyrene−exTTF. Importantly, the spectral pattern of the fluorescence spectrum—with major peaks at 376, 395, and 417 nm—is identical for both samples. This guarantees the chemical and electronic integrity of SWNT-immobilized pyrene−exTTF. On the other hand, a quantitative analysis of the fluorescence quantum yields and, consequently, of the fluorescence quenching is made impossible due to the overwhelming contribution of the plasmonic SWNT absorption in the range of the excitation wavelength.[26]

Strong support for excited-state interactions, in particular between exTTF (i.e., electron donor) and SWNT (i.e., electron acceptor), came from femtosecond transient absorption measurements. Photoexcitation of exTTF and pyrene−exTTF at 387 nm, where pyrene lacks any significant absorption, generates in both cases an exTTF-centered excited state. Spectral characteristics of this very short-lived excited state (1.2 ps) are transient maxima around 465, 605, and 990 nm as well as transient bleaching at <450 nm—see Figure 5.

The short lifetimes (i.e., after 5 ps no transient absorption remains) are rationalized by the presence of the sulfur atoms, with a strong second-order vibronic spin−orbit coupling. Going beyond our femtosecond experiments (i.e., 3 ns) we tested exTTF in nanosecond experiments following 355 nm excitation. However, outside of the 10 ns time window of the instrumental time resolution, no notable transient were detected.

The presence of pyrene (i.e., pyrene−exTTF) exerts no measurable effects on photoexcited exTTF. For example, the excited-state lifetime is still 1.2 ps—see Figure 5—and transient maxima as well as transient bleach evolve at 465 and 605 and 450 nm, respectively. In contrast, nanosecond experiments confirmed that the presence of exTTF causes a rapid deactivation of the pyrene singlet excited state via intramolecular energy transfer interactions from photoexcited pyrene (3.3 eV) to exTTF (2.7 eV) or fast intramolecular electron-transfer interactions to yield a very short-lived radical ion pair state (2.3 eV).

Looking at pristine SWNT, which were simply suspended in THF, a set of transient minima were observed at 1050, 1185, 1310, 1435, and 1555 nm. As Figure 6 shows, all features decay

(26) In time-resolved fluorescence measurements the only detectable component reveals a lifetime of around 16 ns.

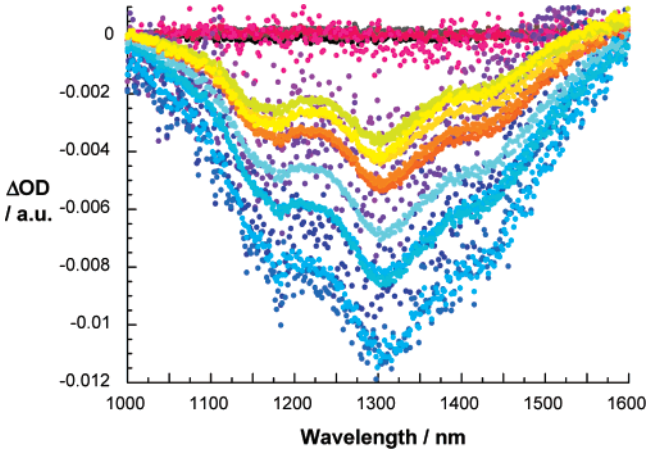

Figure 6. Differential absorption spectra (near-infrared) obtained upon femtosecond flash photolysis (387 nm) of SWNT in THF with several time delays between 0 and 10 ps at room temperature.

similarly to recover the ground state with two major components (i.e., 1.2 and 520 ps), while no particular shifts were observable.

Finally, when photoexciting SWNT/pyrene−exTTF the 605 nm transient decays remarkably fast with a lifetime even shorter than in pyrene−exTTF and exTTF—compare 0.9 with 1.2 ps. Moreover, simultaneous with the pyrene−exTTF excited-state decay, evolution of a product—with a main maximum at 685 nm—is registered. This new transient resembles the radiolytically (Supporting Information Figure S2) and photolytically generated one-electron oxidized exTTF radical cation (Figure 7). The latter figure shows the transient with a 10 ps time delay—a time scale on which all exTTF-centered excited states have returned to the ground state. Additional exTTF radical cation features are bleaching <450 nm and a shoulder at 480 nm, as discernible in the radiolysis of exTTF and the femtosecond photolysis of SWNT/pyrene−exTTF. The band around 530 nm, on the other hand, is due to a SWNT reduced product.[27]

No exTTF radical cation transient absorption has been observed for pyrene−exTTF in the absence of SWNT (vide supra). This is indicative for the existence of strong interaction between SWNT and pyrene−exTTF, which results in fast electron transfer from the photoexcited exTTF to SWNT. Interestingly, SWNT/exTTF electron-transfer interactions seem not to involve pyrene at all, which suggests close interactions between SWNT and exTTF.

Important is also the range beyond 1000 nm (i.e., 1000−1600 nm), which immediately after the photoexcitation is dominated by a negative imprint of the van Hove singularities.[28] These spectral characteristics, although decaying slightly faster than the exTTF transition at 605 nm with 0.8 and 0.78 ps at 1310 and 1170 nm, respectively, transform into a new product. Appreciable blue-shifts of the transient bleaches with minima at 1040, 1150, 1300, 1415, and 1550 nm are detected—see Figure 7 (lower part). Implicit are new conduction band electrons—injected from photoexcited exTTF—shifting the transitions to lower energies. Spectroscopic support for this

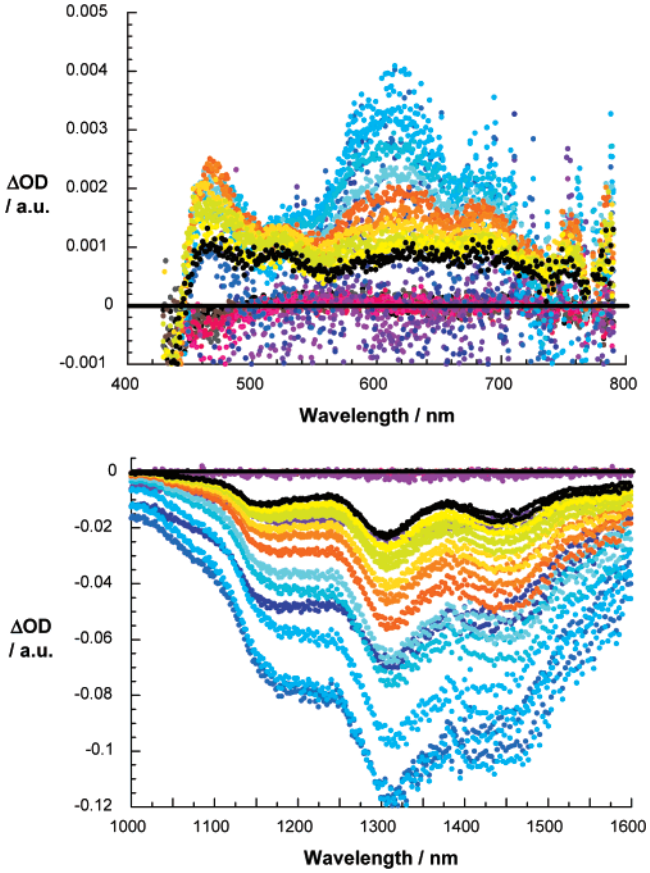

Figure 7. Upper part: differential absorption spectra (visible) obtained upon femtosecond flash photolysis (387 nm) of SWNT/pyrene−exTTF in THF with several time delays between 0 and 10 ps at room temperature. Lower part: differential absorption spectra (near-infrared) obtained upon femtosecond flash photolysis (387 nm) of SWNT/pyrene−exTTF in THF with several time delays between 0 and 10 ps at room temperature.

assumption came from determining the absolute spectrum of the product and comparing it with that of the ground state.[29] As Figure 8 (lower part) illustrates, the van Hove singularities shift indeed to the red. A global analysis of the 1000−1600 nm region—Figure 8 (central part)—resulted in a lifetime of this newly generated radical ion pair state of about 2900 ± 200 ps.

Conclusions

In conclusion, we have demonstrated the successful use of $\pi-\pi$ interactions to anchor an electron-donating exTTF to the surface of SWNT by using a pyrene tether moiety that strongly adsorbs on the surface of SWNT. For the first time a complete and concise characterization of the radical ion pair state has been achieved, especially in light of injecting electrons into the conduction band of SWNT. Furthermore, $\pi-\pi$ interactions between the concave hydrocarbon skeleton of exTTF and the convex surface of SWNT adds further strength and stability to the SWNT/pyrene−exTTF nanohybrid. Because of the close proximity of the exTTF to the electron acceptor SWNT, a very rapid intrahybrid electron transfer affords a photogenerated radical ion pair, whose lifetime is only a few nanoseconds. In fact, much longer lived radical ion pair states have been

(27) Saito, K.; Troiani, V.; Qiu, H.; Solladie, N.; Sakata, T.; Mori, H.; Ohama, M.; Fukuzumi, S. *J. Phys. Chem. C* **2007**, *111*, 1194−1199.

(28) (a) Barone, V.; Peralta, J. E.; Wert, M.; Heyd, J.; Scuseria, G. E. *Nano Lett.* **2005**, *5*, 1621−1624. (b) Spataru, C. D.; Ismael-Beigi, S.; Benedict, L. X.; Louie, S. G. *Phys. Rev. Lett.* **2004**, *92*, 077402(1)− 077402(4). (c) Zhou, Z.; Steigerwald, M.; Hybertsen, M.; Brus, L.; Friesner, R. A. *J. Am. Chem. Soc.* **2004**, *126*, 3597−3607.

(29) The spectrum of the reduced state was determined by simply subtracting the changes—seen in the differential absorption spectrum—from the ground state.

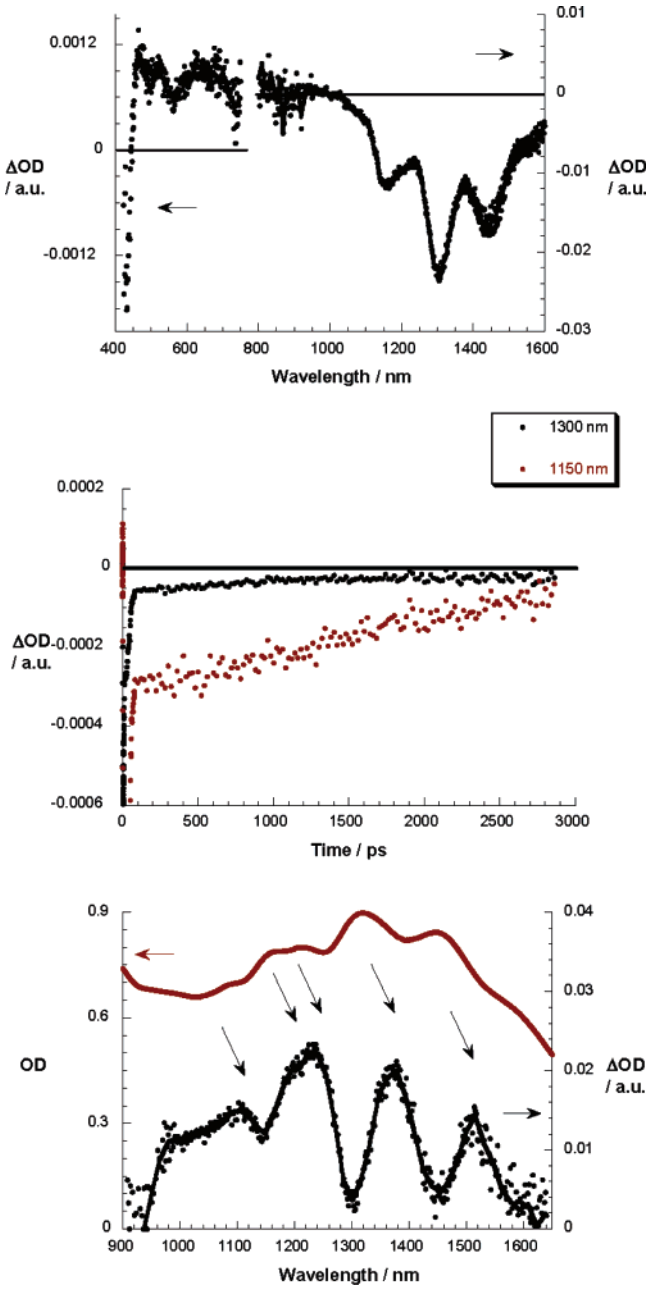

Figure 8. Upper part: differential absorption spectra (visible and near-infrared) obtained upon femtosecond flash photolysis (387 nm) of SWNT/pyrene−exTTF in THF with a 10 ps time delay at room temperature; please note the different *y*-axis scales. Central part: time−absorption profiles of the spectra shown in the upper part at 1150 (i.e., red spectrum) and 1300 nm (black spectrum), monitoring the formation and decay of the radical ion pair state. Lower part: absolute spectra of SWNT/pyrene−exTTF ground (i.e., red spectrum) and reduced (i.e., black spectrum) state in THF; please note the different *y*-axis scales.

generated when the corresponding electron donor moieties are placed at larger distance relative to the SWNT surface, for example, 14 μs in SWNT−PSS/H_2P^{8+} or 1110 ± 100 ns in SWNT−Fc.[7a,c] The present method for the preparation of SWNT/exTTF nanohybrids nicely complements the covalent approach[9a] and bears a strong promise for the preparation of systems for photoinduced energy conversion based on electroactive tweezers, in which the pyrene moiety acts as an efficient template for the supramolecular organization of SWNT-based donor−acceptor complexes.

Experimental Section

General. All solvents were dried and distilled according to standard procedures. Reagents were used as purchased. 2-(Hydroxymethyl)-9,10-bis(1,3-dithiol-2-ylidine)-9,10-dihydroanthracene (exTTF) was obtained by a previously reported procedure.[21] Flash chromatography was performed using silica gel (Merck, Kieselgel 60, 230−240 mesh o Scharlau 60, 230−240 mesh). Analytical thin layer chromatography (TLC) was performed using aluminum-coated Merck Kieselgel 60 F254 plates. An Agilent 1100 series LC module (HPLC) system, equipped with a diode array detector, was used to determine the purity of the pyrene−exTTF compound synthesized. A semipreparative SiO_2 column (column dimensions, 25 cm × 10 mm; flow rate, 2.0 mL min^{-1}; injection volume, 20 μL; mobile phase, toluene) was employed. The retention time (t_R) and the peak area (PA) reported were determined at a wavelength of 305 nm. Melting points were measured on a Thermolab apparatus. NMR spectra were recorded on a Bruker AC-200 (^{1}H, 200 MHz; ^{13}C, 50 MHz) spectrometer at 298 K using partially deuterated solvents as internal standards. Coupling constants (J) are denoted in Hz, and chemical shifts (δ) are in ppm. Multiplicities are denoted as follows: s = singlet, d = doublet. IR spectra were recorded on a Perkin-Elmer 257. UV−vis or UV−vis−NIR spectra were recorded with a Varian Cary 50 or a Varian Cary 5000 spectrophotometer by using CH_2Cl_2 or THF as solvents. Raman spectra at 1064 nm were taken on a LabRam HR Raman microscope from Jobin Yvon. Matrix-assisted laser desorption ionization (coupled to a time-of-flight analyzer) experiments (MALDI-TOF) were recorded on a 4700 Reflector spectrometer.

TEM Analysis. A small amount of the SWNT/pyrene−exTTF sample was suspended in DMF, and a drop of the suspension was placed on a copper grid (3.00 mm, 200 mesh, coated with carbon film). After air-drying the sample was investigated by a TEM Philips EM 208, with an accelerating voltage of 100 kV.

AFM Analysis. The samples were prepared by spin coating on silicon wafers from a solution of SWNT/pyrene−exTTF in DMF and then investigated with a Veeco Multimode scanning probe microscope equipped with a Nanoscope IIIa controller.

TGA Analysis. A solution of SWNT/pyrene−exTTF was centrifuged at 6000 rpm for 4 h, the supernatant was removed, and the solid was dried under vacuum overnight. The thermogravimetric analyses were performed with a TGA Q500 TA instrument at 10 °C/min under nitrogen.

Electrochemical Measurements. The solution electrochemistry of the pyrene−exTTF compound and SWNT/pyrene−exTTF mixtures was investigated by CV and OSWV in deoxygenated CH_2Cl_2 and THF containing tetra-*n*-butylammonium perchlorate ($TBAClO_4$) (0.1 M) as supporting electrolyte. A single-compartment, three-electrode cell configuration was used in this work. A glassy carbon electrode (3 mm diameter) was used as the working electrode, a platinum wire as the counter, and a Ag wire in a 0.01 M $AgNO_3$/0.1 M $TBAClO_4$–CH_3CN solution as the reference electrode. All electrochemical measurements were performed with a AUTOLAB potentiostat/galvanostat with PGSTAT30 equipped with a software GPES for windows version 4.8.

Photophysical Measurements. Femtosecond transient absorption studies were performed with 387 nm laser pulses (1 kHz, 150 fs pulse width) from an amplified Ti:sapphire laser system (Clark-MXR, Inc.). For all photophysical experiments an error of 10% must be considered. Fluorescence spectra were recorded with a FluoroMax. The experiments were performed at room temperature. Each spectrum was an average of at least five individual scans, and the appropriate corrections were applied. Pulse radiolysis experiments were accomplished using 50 ns pulses of 8 MeV electrons from a model TB-8/16-1S electron linear accelerator.

Synthesis of 4-Pyrene-1-ylbutyric Acid 9,10-Bis[1,3]dithiol-2-ylidene-9,10-dihydroanthracen-2-ylmethyl Ester (Pyrene−exTTF). To 20 mL of CH_2Cl_2 was added 2-(hydroxymethyl)-9,10-bis(1,3-dithiol-

2-ylidene)-9,10-dihydroanthracene (exTTF)[21] (0.85 mmol) and 1-pyrenebutyric acid (1.20 mmol). The mixture was stirred for 10 min at 0 °C (ice/water bath) under N_2. Then 1,3-dicyclohexylcarbodiimide (DCC) (1.20 mmol) and 4-(dimethylamino)-pyridine (DMAP) (0.12 mmol) in 5 mL of CH_2Cl_2 were added, and the mixture was stirred for another 15 min at 0 °C. The cooling bath was then removed, and the solution was allowed to warm to room temperature. After being stirred for 24 h under N_2, the reaction mixture was washed with water (3 × 50 mL). The organic layer was dried over $MgSO_4$, filtered, and evaporated. The residue was subjected to column chromatography in hexane/AcOEt 3/1 for further purification. Yield: 96%. HPLC (analytical) $t_R = 9.35$ min, PA = 99%. mp: 147−149 °C. IR (KBr): 2928, 2854, 1728 (CO), 1544, 1511, 1453, 1256, 1159, 843, 756, 646 cm^{-1}. ^1H NMR (200 MHz, $CDCl_3$) δ: 8.17 (1H, d, $J = 9.30$ Hz), 8.14−7.94 (7H, m), 7.83 (1H, d, $J = 8.06$ Hz), 7.72−7.65 (4H, m), 7.31−7.26 (3H, m), 6.26 (1H, AB, $J_{AB} = 6.80$ Hz), 6.24 (1H, AB, $J_{AB} = 6.80$ Hz), 6.18 (1H, AB, $J_{AB} = 6.60$ Hz), 6.06 (1H, AB, $J_{AB} = 6.60$ Hz), 5.21 (2H, s), 3.40 (2H, t, $J = 7.80$ Hz), 2.56 (2H, t, $J = 7.80$ Hz), 2.24 (2H, t, $J = 7.8$ Hz). ^{13}C NMR (50 MHz, $CDCl_3$), δ: 173.4 (CO), 136.2, 135.7, 135.6, 135.3, 135.2, 133.6, 131.4, 130.9, 129.9, 128.7, 127.5, 127.4, 127.3, 126.6, 126.0, 125.8, 125.1, 125.0, 124.9, 124.8, 124.7, 124.6, 123.3, 121.7, 117.2, 117.1, 117.0, 116.9, 66.1, 34.0, 32.8, 26.8. M.S. (MALDI-TOF) *m*/*z*: calcd for $C_{41}H_{28}O_2S_4 = 680.0967$; found = 680.0976. UV−vis (CH_2Cl_2) λ_{max} (log ϵ): 433 (4.25), 413 (4.18), 367 (4.06), 346 (4.62), 329 (4.46), 315 (4.15), 278 (4.67), 268 (4.48), 243 (4.85) nm.

Acknowledgment. This work was supported by the MEC of Spain (project CTQ2005-02609/BQU), the CAM (project P-PPQ-000225-0505), the University of Trieste and MUR (PRIN 2006, prot. 2006034372), the Deutsche Forschungs-Gemeinschaft (SFB 583), FCI, and the Office of Basic Energy Sciences of the U.S. Department of Energy. This is contribution NDRL-4758 from the Radiation Laboratory. M.A.H. and M.G. thank the MEC of Spain for a Ramón y Cajal contract and an FPU Grant, respectively. C.E. acknowledges a Grant from the 21st Century COE program of Osaka University.

Supporting Information Available: Raman spectra, differential absorption spectrum (visible) monitored 200 μs after pulse radiolytic oxidation of exTTF in oxygenated dichloromethane solutions, ^1H NMR, ^{13}C NMR, and MALDI-TOF mass spectrum. This material is available free of charge via the Internet at http://pubs.acs.org.

JA073975T